

Zubair Akhter*, Pankaj Kumar and M. Jaleel Akhtar

Sub-Surface Microwave Imaging Using Four-Slot Vivaldi Antenna with Improved Directivity

DOI 10.1515/freq-2016-0054

Received February 25, 2016

Abstract: The conventional tapered slot Vivaldi antenna is well known for its ultra-wide band characteristics with low directivity. To improve the directivity of the conventional Vivaldi antenna, a four-slot Vivaldi antenna (FSVA) is proposed here to operate in the frequency range of 2–11 GHz. For feeding the FSVA, a binomial three-section V-shaped even mode power divider with progressing T-junctions is also designed and tested here, which is then integrated with the antenna. The proposed antenna prototype is designed and fabricated on a 1-mm thick FR-4 substrate ($\epsilon_r = 4.3$, $\tan\delta = 0.025$), and the return loss and radiation characteristics are investigated in the anechoic environment. The measured result shows a good agreement with the numerical simulation performed using the EM Simulator i. e. CST MWS-2015. It is found that the directivity of FSVA is approximately doubled as compared to that of the conventional Vivaldi antenna having the same dimensions. From the application point of view, the fabricated antenna is used to image various metallic objects hidden inside the sand using a vector network analyzer and associated RF components. The obtained 2D microwave images of the test media successfully show that the hidden objects can effectively be located and detected using the proposed FSVA in conjunction with a simple imaging scheme.

Keywords: microwave imaging, NDT, TSVA, UWB antenna, Vivaldi antenna, V-shaped power divider

1 Introduction

The traditional Vivaldi antenna, also known as the tapered slot Vivaldi antenna (TSVA) was first proposed by Gibson in 1979 [1]. The ultra-wide band (UWB) characteristic of the TSVA results into numerous applications

in various fields such as microwave imaging [2], vehicular communication [3], radio astronomy [4] and high speed communication systems. It is a preferred choice over the horn antenna especially for microwave imaging and non-destructive testing (NDT) due to ease of fabrication in planar technology, low cost, ultra-wide bandwidth and relatively small size. However, one of the bottlenecks of the conventional Vivaldi antenna has been its relatively low directivity. In order to improve its far field characteristic such as the directivity, various methods have been proposed employing array design [5]–[7], loading zero index metamaterials (ZIM) [8]–[10], placing dielectric lens in front of the antenna [11], employing a director at the aperture of the antenna [12], a palm tree approach [13] etc. Recently, a double-slot Vivaldi antenna has been proposed to improve the directivity by certain factor [14]. However, the directivity of some of the double-slot Vivaldi antennas reported in the literature is not significantly high [10].

The aim of this paper is to propose a four-slot Vivaldi antenna (FSVA) so that the directivity can be significantly increased to make the antenna more useful for microwave imaging and NDT applications. The overall concept can be made valid for the multi-slot Vivaldi antenna design, and hence a comprehensive study is carried out here to improve the directivity of conventional Vivaldi antenna. The design methodology of the multi-slot Vivaldi antenna can be considered to be different from the conventional TSVA design in some aspects as its overall size is usually less than a wavelength [14]–[18].

For the feeding of multi-slot antenna, various types of power dividers such as the T-junction power divider [19], the Wilkinson power divider [20], and the substrate integrated waveguide (SIW) power divider [7] have been reported. However, the Wilkinson and SIW power dividers are not suitable for UWB applications due to relatively less impedance bandwidth. Hence, a three section simple V-shaped power divider using the binomial transformation is designed and proposed here to feed the proposed four-slot Vivaldi antenna.

The proposed four-slot Vivaldi structure is responsible for almost uniform field distribution at the aperture which shows high directivity as compared to the earlier proposed ZIM loaded Vivaldi antenna [8] and double-slot

*Corresponding author: Zubair Akhter, Department of Electrical Engineering, Indian Institute of Technology, ACES 117, Academic Area, Kanpur, Uttar Pradesh, India, E-mail: zuakhter@iitk.ac.in
Pankaj Kumar, M. Jaleel Akhtar, Department of Electrical Engineering, Indian Institute of Technology, ACES-326, Academic Area, Kanpur, Uttar Pradesh, India

antenna [10] of approximately the same size. The design methodology of the multi slot antenna is chosen in such a way that the beam splitting at higher frequency can be avoided, which results into the directivity improvement from 7 dBi to 13.5 dBi as compared to the conventional ZIM loaded TSVA [2] with same dimension over the frequency range of 2–11 GHz.

2 Design of four-slot antenna and power divider

2.1 Design of four-slot Vivaldi antenna

In this section, the basic geometry configurations of the TSVA [2] and the proposed FSVA with front and back views are shown in Figures 1 and 2, respectively.

The proposed FSVA is designed on a 1-mm thick FR-4 substrate ($\epsilon_r = 4.3$, $\tan\delta = 0.025$) and the geometry and dimensions of ZIM cell loaded TSVA are also given here for comparison.

The various exponential curves of the proposed FSVA antenna as shown in Figure 2 can be expressed using the following relations,

$$E_{s1} : y = \frac{1}{2} \left(W_{F3} - W_F * \exp \left(\ln \left(\frac{W_{F3}}{W_F} \right) * \frac{x}{L_{F2}} \right) \right) \quad (0 \leq x \leq L_{F2}) \quad (1)$$

$$E'_{s1} : y = -\frac{1}{2} \left(W_{F3} - W_F * \exp \left(\ln \left(\frac{W_{F3}}{W_F} \right) * \frac{x}{L_{F2}} \right) \right) \quad (0 \leq x \leq L_{F2}) \quad (2)$$

$$E_{s2} : y = \frac{1}{2} \left(W_{F3} + W_F * \exp \left(\ln \left(\frac{W_{F3}}{W_F} \right) * \frac{x}{L_{F2}} \right) \right) \quad (0 \leq x \leq L_{F2}) \quad (3)$$

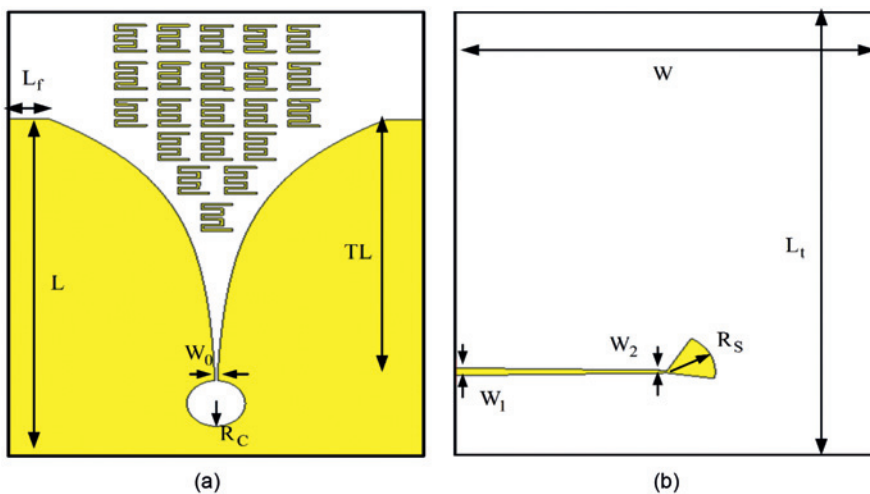


Figure 1: Simulated TSVA design (a) front view (b) back view.

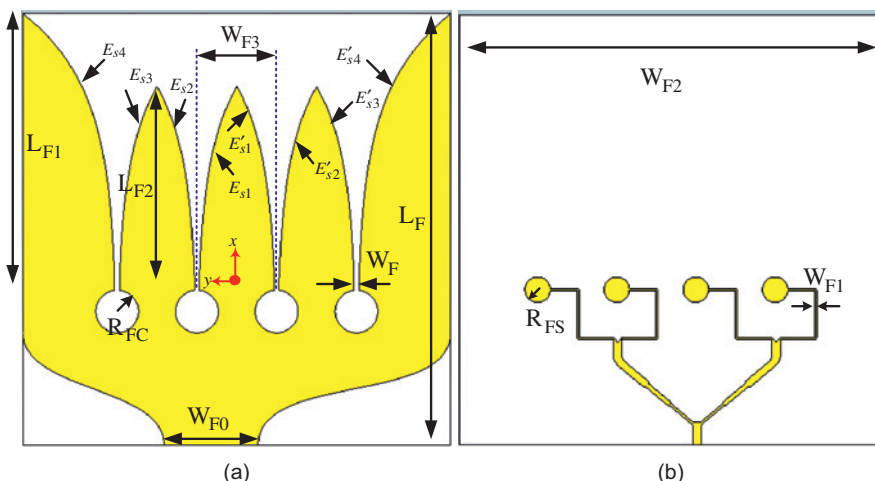


Figure 2: Proposed FSVA design (a) front view (b) back view.

$$E'_{s2} : y = -\frac{1}{2} \left(W_{F3} + W_F * \exp \left(\ln \left(\frac{W_{F3}}{W_F} \right) * \frac{x}{L_{F2}} \right) \right) \quad (0 \leq x \leq L_{F2}) \quad (4)$$

$$E'_{s3} : y = \frac{1}{2} \left(3 W_{F3} - W_F * \exp \left(\ln \left(\frac{W_{F3}}{W_F} \right) * \frac{x}{L_{F2}} \right) \right) \quad (0 \leq x \leq L_{F2}) \quad (5)$$

$$E'_{s3} : y = -\frac{1}{2} \left(3 W_{F3} - W_F * \exp \left(\ln \left(\frac{W_{F3}}{W_F} \right) * \frac{x}{L_{F2}} \right) \right) \quad (0 \leq x \leq L_{F2}) \quad (6)$$

$$E'_{s4} : y = \frac{1}{2} \left(3 W_{F3} + W_F * \exp \left(\ln \left(\frac{W_{F2} - 3 W_{F3}}{W_F} \right) * \frac{x}{L_{F1}} \right) \right) \quad (0 \leq x \leq L_{F1}) \quad (7)$$

$$E'_{s4} : y = -\frac{1}{2} \left(3 W_{F3} + W_F * \exp \left(\ln \left(\frac{W_{F2} - 3 W_{F3}}{W_F} \right) * \frac{x}{L_{F1}} \right) \right) \quad (0 \leq x \leq L_{F1}) \quad (8)$$

The final design parameters of both the antennas are tabulated in Tables 1 and 2 respectively.

Table 1: Parameters of TSVA.

Parameters	L	W	R _C	R _S	W ₀	W ₁	W ₂	L _t	L _f	T _L
Value(mm)	80	105	6.5	7.3	1	1.96	0.25	95	15	66

Table 2: Parameters of FSVA.

Parameters	L _F	L _{F1}	L _{F2}	W _F	W _{F0}	W _{F1}	W _{F2}	W _{F3}	R _{FS}	R _{FC}
Value(mm)	92	57	42.25	1	20	0.45	90.6	16.90	2.7	4.5

It can be observed from Figures 1 and 2 that the overall size of the proposed four-slot Vivaldi antenna is almost the same as that of the ZIM loaded tapered slot Vivaldi antenna although the directivity of four-slot antennas is improved significantly.

2.2 Design of V-shaped power divider

The schematic of proposed V-shaped power divider with three sections is shown in Figure 3. The proposed geometry is designed over FR-4 ($\epsilon_r = 4.3$, $\tan\delta = 0.025$)

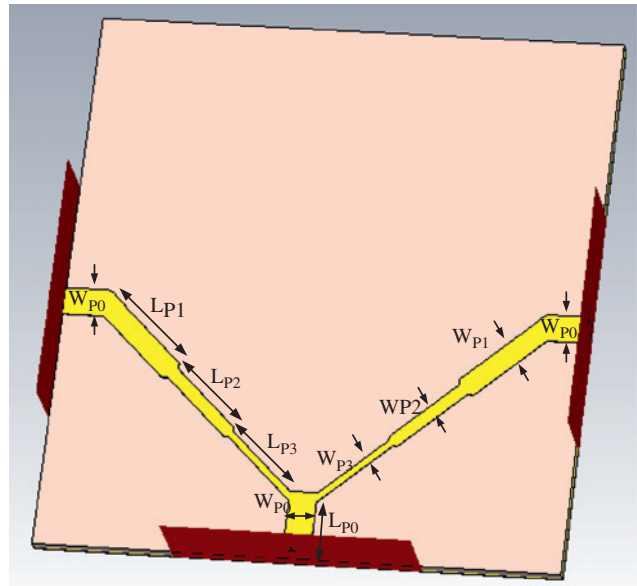


Figure 3: Schematic of V-shaped power divider.

substrate of 1 mm thickness. The characteristic impedances of $\lambda/4$ sections have been evaluated using the following equations [21].

$$\ln \frac{Z_{n+1}}{Z_n} = 2^{-N} C_n^N \ln \frac{Z_L}{Z_0} \quad (9)$$

$$C_n^N = \frac{N!}{(N-n)!n!} \quad (10)$$

where C_n^N are the binomial coefficients and N represent the number of section. The above relations are used for $N=3$, $n=0$ to $N-1$ and $Z_0=50 \Omega$, $Z_L=100 \Omega$. The optimized parameters of the power divider are shown in Table 3.

Table 3: Optimized parameters of V-shaped power divider.

Impedance	50 Ω		54.5 Ω		70.7 Ω		91.7 Ω	
	W _{P0}	L _{P0}	W _{P1}	L _{P1}	W _{P2}	L _{P2}	W _{P3}	L _{P3}
Values(mm)	1.96	5	1.58	6.4	0.96	6.4	0.51	6.4

3 Results and discussion

The first step in the design of UWB antenna is the design of feeding/matching network working over a wide band, which is considered to be extremely challenging problem. For the feeding of proposed FSVA, a V-shaped ultra-wide band power divider is designed for the frequency range of 2–11 GHz, which is then integrated with the proposed four-slot antenna as shown in Figure 2.

The performance of the designed V-shaped power divider is shown in Figure 4. It can be observed from Figure 4(a) that the input power from port 1 is divided equally between port 2 and port 3 as both S21 and S31 are showing values of -3 dB over the entire frequency range. It can similarly be noted from Figure 4(b) that the output signals from port 2 and port 3 are in the same phase as the phase plots of both S21 and S31 are matching over the desired frequency range.

Further, each coupled port (i. e., port 2 and port 3) is followed by a T-junction in order to excite all the four slots of the proposed antenna. The fabricated prototype of the FSVA is shown in Figure 5. The V-shaped power divider is an integral part of the proposed FSVA as seen in Figure 5(b). The reflection coefficient of the designed FSVA is measured in the electromagnetic anechoic

environment as shown in Figure 6 using the Agilent (N5320C) vector network analyzer.

The return loss (simulated and measured) of the proposed FSVA for the frequency range of 2–11 GHz is shown in Figure 7. It can be observed that the return loss is more than 10 dB over the entire operating range of the antenna. The deviation between the simulated and the measured S11 data could be due to many factors including the fabrication tolerances. However, one of the major reasons for this deviation may be due to the use of FR-4 substrate as the FR-4 is usually modeled as a constant permittivity material over the entire frequency band. But, in real situation, the value of FR-4 permittivity might change over the operating frequency band which could lead to some deviation between the simulated and the measured S11.

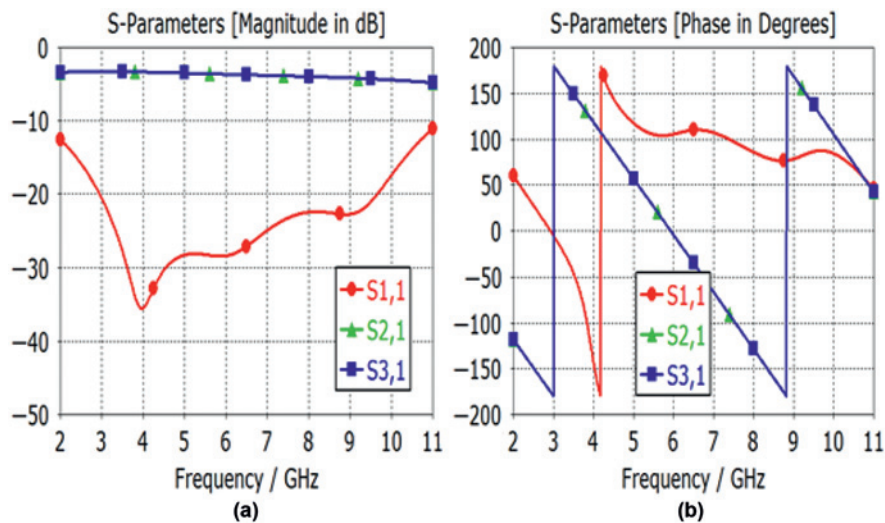


Figure 4: Simulated S-parameters
(a) magnitude (b) phase of the
designed V-shaped power divider.

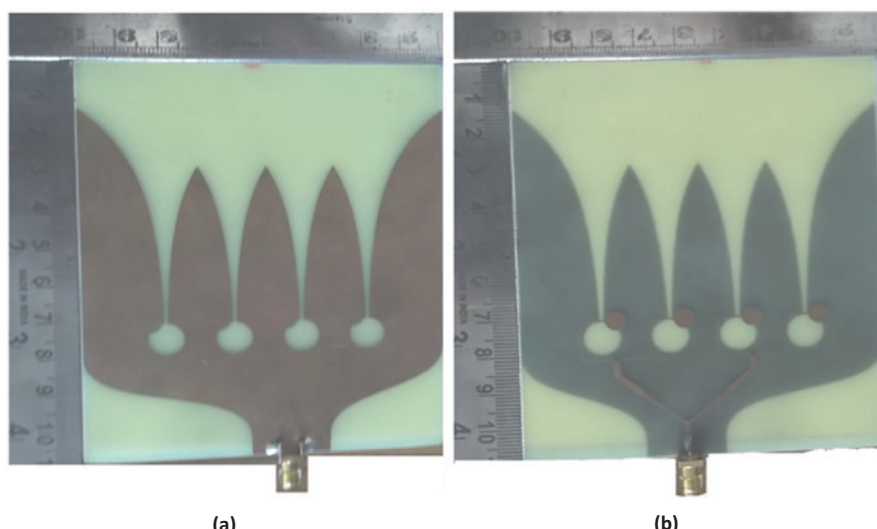


Figure 5: Fabricated FSVA (a) front view
(b) back view.

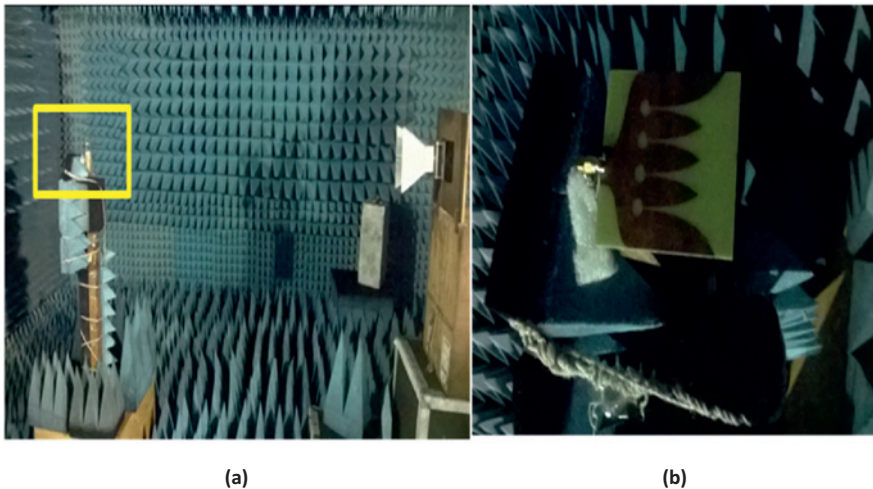


Figure 6: Measurement environment
 (a) experimental setup for testing of the designed antenna (b) incite showing top view of the testing antenna.

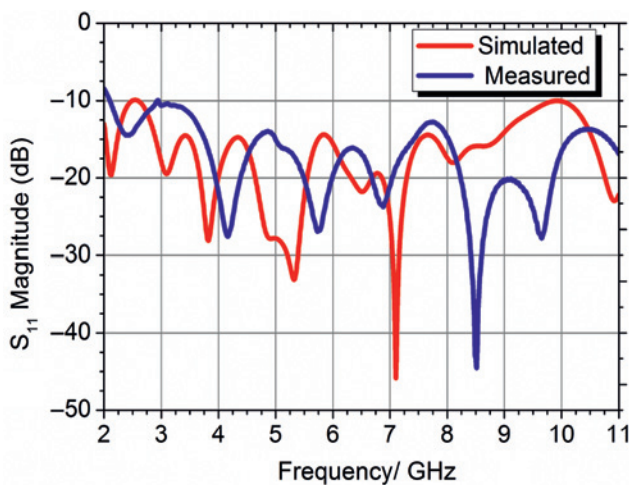


Figure 7: Simulated and measured return loss of FSVA.

It is to be noted that the proposed four-slot Vivaldi antenna shows significant improvement in directivity as compared to that of the conventional TSVA due to focusing slots at the aperture of antenna which produced plane like wave as shown in Figure 8.

A comparison of simulated directivity, simulated peak realized gain and measured peak realized gain is carried out as shown in Figure 9. It is observed from this figure that the maximum directivity of the proposed FSVA reaches up to 13.5 dBi whereas the measured value of the realized gain approached 11 dBi at 7.6 GHz with its values ranging from 3.75 to 11 dBi in the frequency band of 2–11 GHz, which is quite attractive for microwave imaging applications. It is to be noted here that the proposed antenna shows somewhat low directivity in the lower frequency range (below 6 GHz). This could be due to the fact that at lower frequencies, the

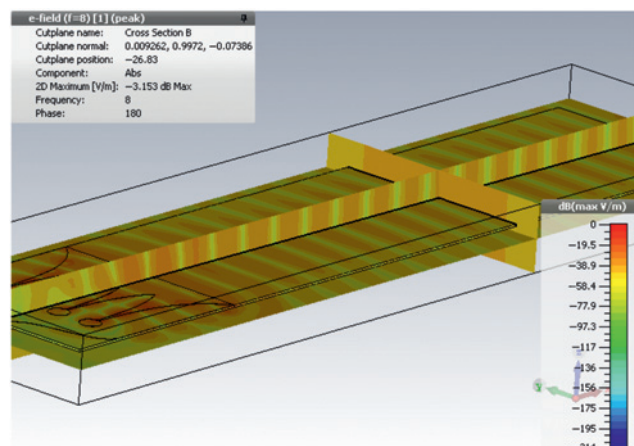


Figure 8: Simulated E-field distribution at 8 GHz.

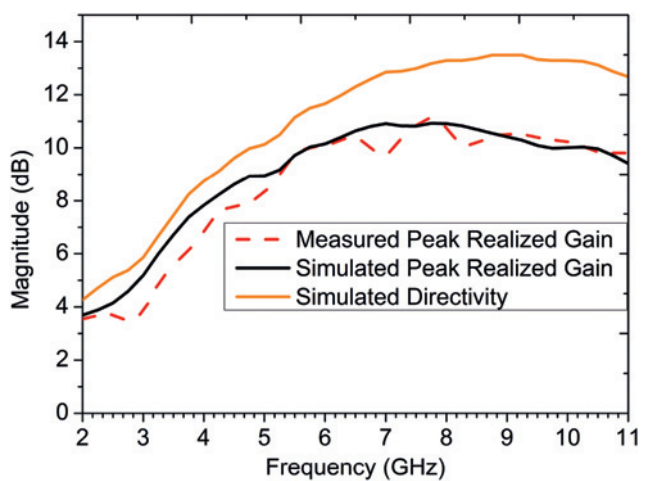


Figure 9: Comparison of measured and simulated peak realized gain with simulated directivity.

radiation occurs primarily from the outer edge of the designed Vivaldi antenna and hence the beam is diverging and is not very directive. Additionally, the simulated and measured E-plane /H-plane radiation patterns for different frequencies are plotted here as shown in

Figures 10 and 11. It can be observed from these radiation pattern plots that a good agreement is achieved between the simulated and measured data for all the cases, which verifies the design of the proposed four-slot Vivaldi antenna.

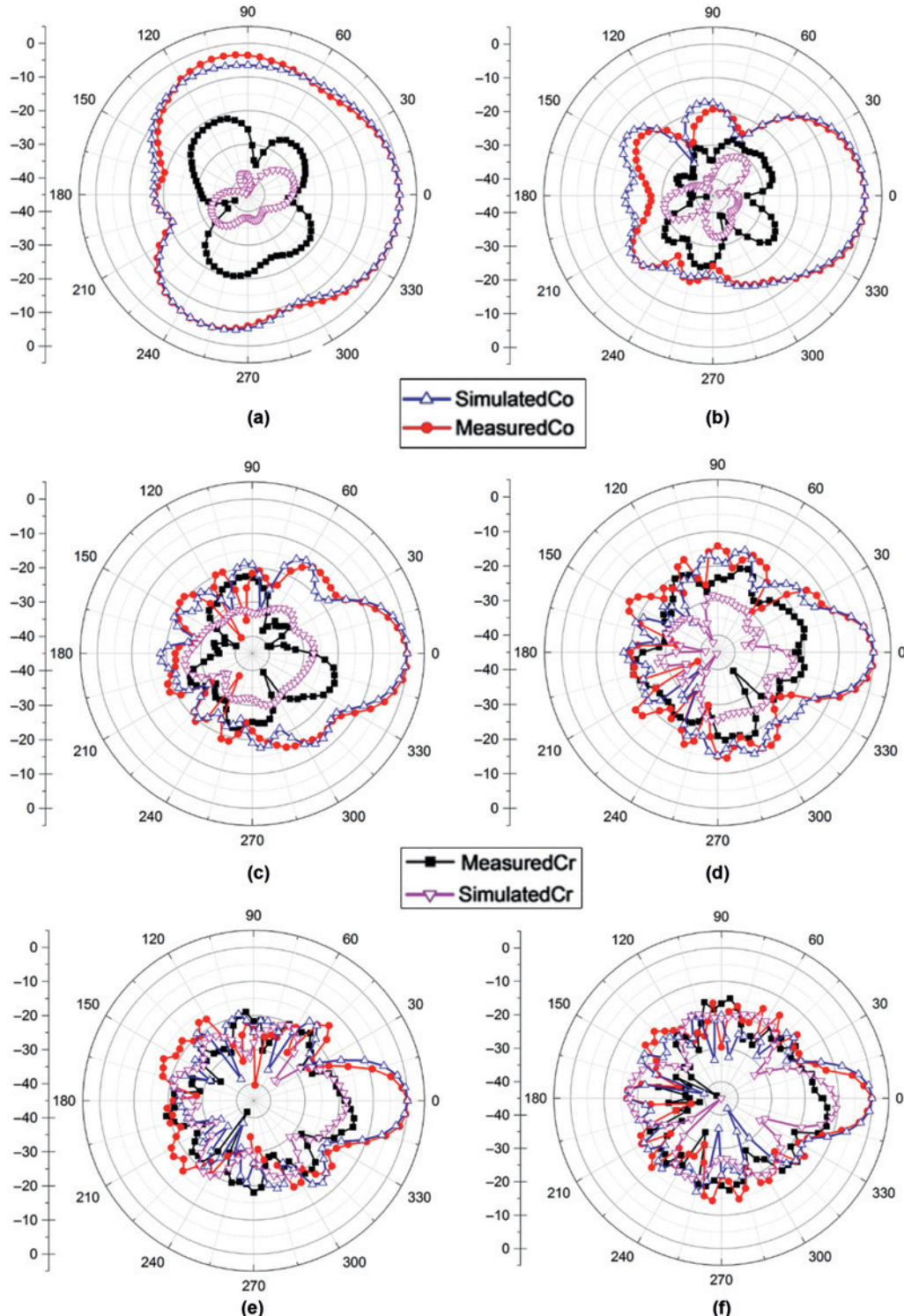


Figure 10: Comparison of measured and simulated E-plane radiation patterns ($\theta = 90^\circ$) at (a) 2 GHz (b) 4 GHz (c) 6 GHz (d) 8 GHz (e) 10 GHz (f) 11 GHz.

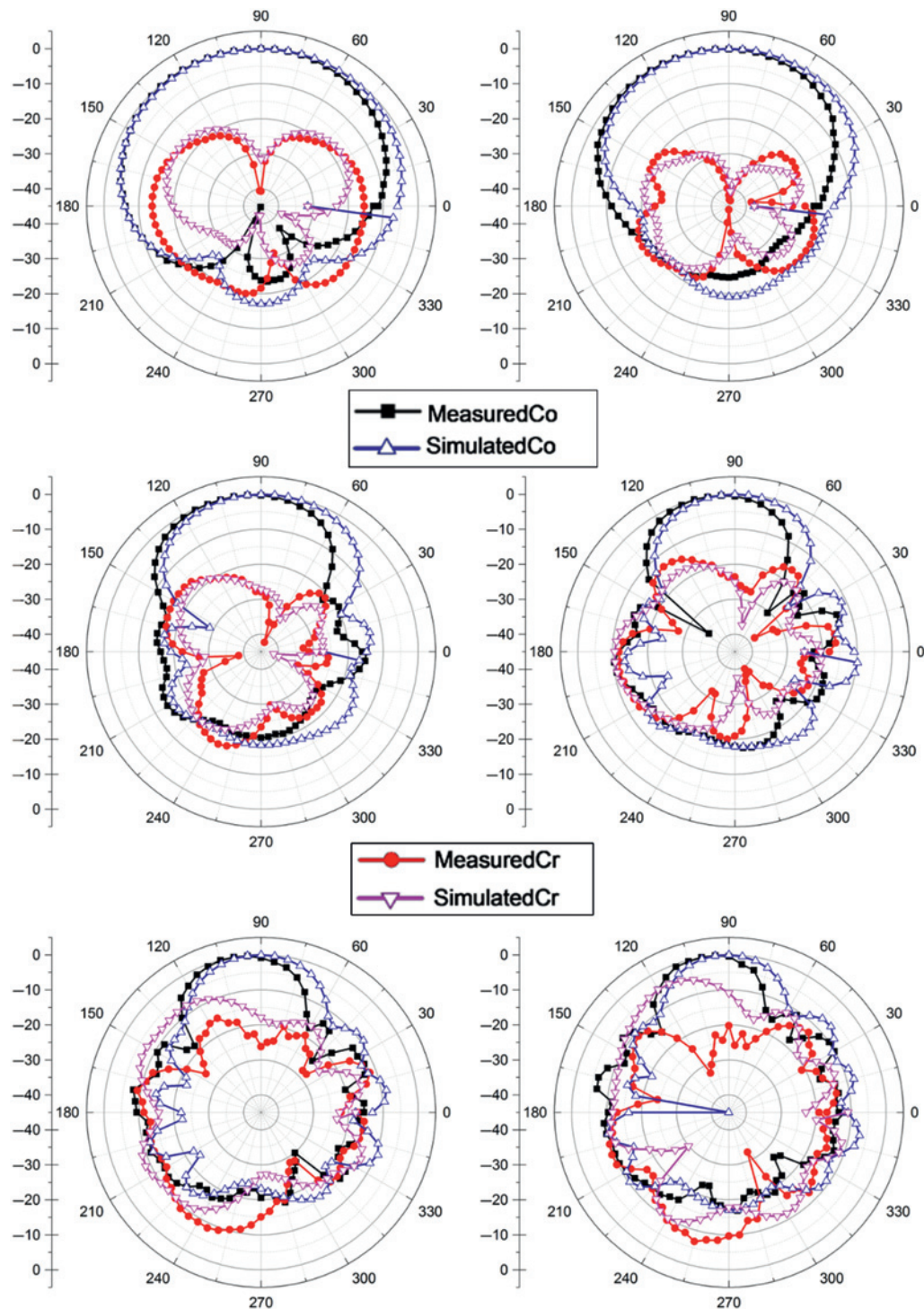


Figure 11: Comparison of measured and simulated H-plane radiation patterns ($\phi = 0^\circ$) at (a) 2 GHz (b) 4 GHz (c) 6 GHz (d) 8 GHz (e) 10 GHz (f) 11 GHz.

4 Application of FSVA in microwave imaging

As discussed in the last section, the proposed FSVA is having operating frequency ranging from 2–11 GHz with attractive directional characteristics, which is quite suitable for microwave imaging applications [22], [23]. Hence, after validating the proposed antenna design, it is employed in a measurement setup used for the microwave imaging. The microwave imaging setup consists of a vector network analyzer (VNA) along with RF cables and connectors, and an automated x-y scanner as shown in Figure 12.

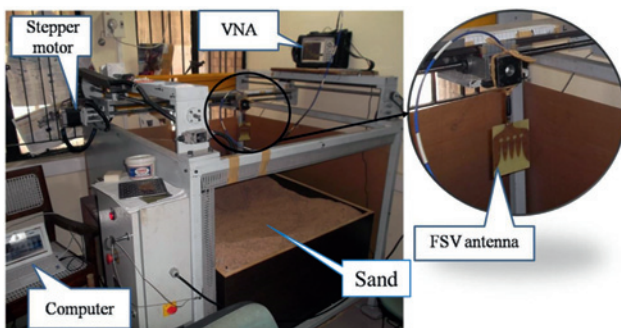


Figure 12: Measurement setup used for microwave imaging.

The main objective here is to locate hidden objects within the box filled with the sand as seen in Figure 12. In order to facilitate the behind the scene imaging, a series of measurements are carried out. In the first step, a reference metal plate is placed on the surface of the test media i.e., sand, which results into complete reflection. Thus the single high peak is observed on the time domain reflectometer (TDR) screen. The TDR here refers to the VNA for visualization of the reflected signal into effective time domain, which is obtained by transforming the wide-band frequency band data with the help of in-built IFFT routines. It is to be noted that the rectangular window is used here for all the

frequency to time domain conversions. After carrying out the reference measurement, the metal plate from the surface is removed and two metallic test objects with dimensions $12\text{ cm} \times 12\text{ cm} \times 1\text{ cm}$ and $8\text{ cm} \times 12\text{ cm} \times 1\text{ cm}$ are concealed inside the sand at depth of 10 cm. The reflection coefficient is measured from the top with the help of an automated scanning setup at a number of points on the investigating domain as shown in Figure 12. When the designed four-slot Vivaldi antenna is positioned over the region where only sand is present, only one reflection peak is usually observed due to the interface between the air and sand. However, when the antenna is positioned over the region containing hidden metallic objects during the scanning procedure, two reflection peaks are clearly observed on the TDR screen. The first peak corresponds to interface between the air and sand, while the second peak occurs due to the interface between the sand and hidden metallic object. Then, the magnitude of obtained reflection peaks have been plotted with the help of *imagesc* command of Matlab. Additionally, the interpolation function *imresize* of the Matlab is used to smoothen the image. The step by step procedure to obtain the microwave reflectivity image of the test media using the proposed FSVA can be explained as follows.

In the first step, the background reflectivity image corresponding to sand area of dimension $60\text{ cm} \times 60\text{ cm}$ is reconstructed as shown in Figure 13. It is noticed here that the background is not homogenous and it shows certain reflectivity pattern which could be due to the presence of some coarse particles inside the sand. In the second step, the reflectivity image corresponding to the situation, when the metallic objects are hidden inside the sand, is obtained as shown Figure 14. Finally, in order to minimize the effects of background media on the actual image of the test object, the image obtained in the first step is subtracted from the image obtained after the second step. This procedure can be considered as the extra processing step which helps in obtaining the sharper image of the test media and compensates for the inhomogeneous nature of sand

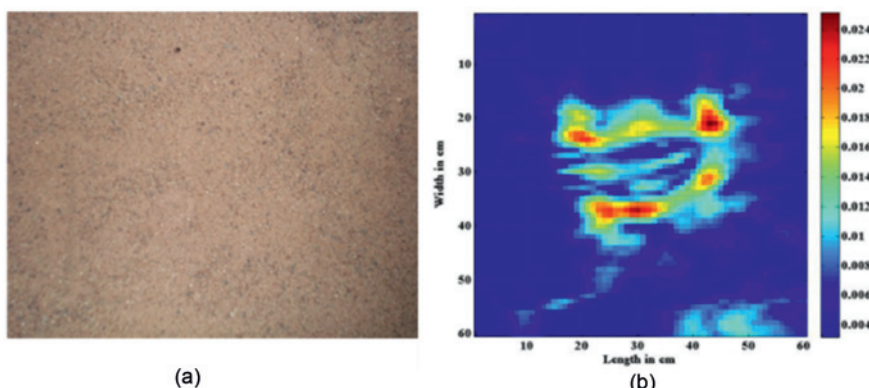


Figure 13: (a) Background sand media
(b) the reflectivity image of the background media.

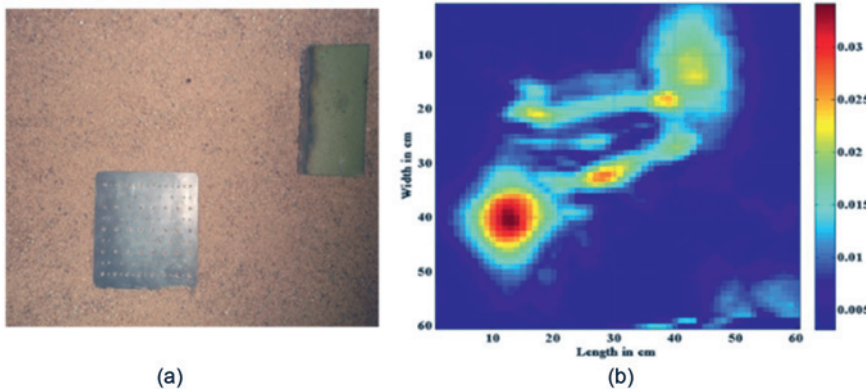


Figure 14: (a) The test objects hidden inside the sand at depth of 10 cm
(b) the raw reflectivity image of the test media containing hidden objects.

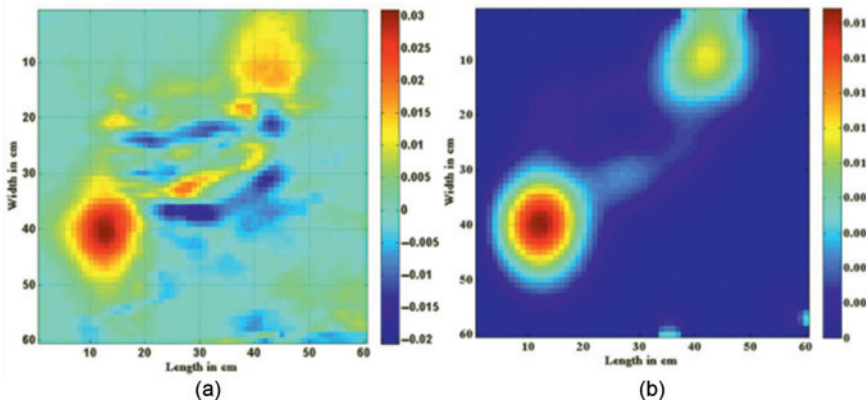


Figure 15: (a) After background image subtraction (b) after averaging.

The final subtracted image of the test media containing hidden objects is shown in Figure 15(a), which is further improved with the help of averaging using MATLAB based standard algorithm as shown in Figure 15(b). It is to be noted that for all the cases, the resolution along the depth of the object would depend upon the bandwidth of the measured data while the lateral resolution would primarily depend upon the antenna's beamwidth.

5 Conclusion

In this work, a novel four-slot Vivaldi antenna (FSVA) for microwave imaging applications has been proposed. To this end, a V-junction power divider using three-section binomial transformer has also been designed and tested which has then been employed to feed the designed antenna. A significant improvement in directivity and beam-width (6 dB and 40° respectively) has been observed as compared to the conventional tapered slot Vivaldi antenna (TSVA). The proposed four-slot Vivaldi antenna has ultimately been used to image closely spaced objects hidden inside the test media. Based on

the results, it can be concluded that the proposed FSVA has potential to be used for broadband applications such as radar and microwave imaging, microwave material characterization and high speed communication systems.

References

- [1] P. J. Gibson, "The Vivaldi aerial," in *9th IEEE European Microwave Conf.*, Brighton, UK, pp. 101–105, 1979, Sep. 17–20.
- [2] M. Bhaskar, E. Johari, Z. Akhter, and M. J. Akhtar, "Design of anisotropic zero-index metamaterial loaded tapered slot Vivaldi antenna for microwave imaging," in *IEEE Antennas and Propagation Society Int. Symp. (APS-URSI)*, Memphis, Tennessee, pp. 1594–1595, 2014, July 6–11.
- [3] S. H. He, "An improved Vivaldi antenna for vehicular wireless communication systems," *IEEE Antennas Wirel. Propag. Lett.*, vol. 13, pp. 1505–1508, 2014.
- [4] E. W. Reid, L. O. Balbuena, A. Ghadiri, and K. Moez, "A 324-element Vivaldi antenna array for radio astronomy instrumentation," *IEEE Trans. Instrum. Meas.*, vol. 61, pp. 241–250, 2012.
- [5] J. Shin and D. H. Schaubert, "A parameter study of stripline-fed Vivaldi notch-antenna arrays," *IEEE Trans. Antennas Propag.*, vol. 47, pp. 879–886, 1999.

- [6] D. H. Schaubert, S. Kasturi, A. O. Borysenko, and W. M. Elsallal, "Vivaldi antenna arrays for wide bandwidth and electronic scanning," in *2nd European Conf. Antennas and Propagation (EuCAP)*, Edinburgh, Scotland, pp. 1–6, 2007, Nov. 11–16.
- [7] R. Kazemi and A. E. Fathy, "16-element Vivaldi antenna array fed by a single ridge substrate integrated waveguide with over 75% bandwidth," in *IEEE MTT-S Int. Microwave Conf. (IMS)*, Tampa, Florida, pp. 1–4, 2014, June 1–6.
- [8] M. Bhaskar, E. Johari, Z. Akhter, and M. J. Akhtar, "Gain enhancement of the Vivaldi antenna with band notch characteristics using zero-index metamaterial," *Microw. Opt. Technol. Lett. (MOTL)*, vol. 58, pp. 233–238, 2016.
- [9] Z. Bin and T. J. Cui, "Directivity enhancement to Vivaldi antennas using compactly anisotropic zero-index metamaterials," *IEEE Antennas Wirel. Propag. Lett.*, vol. 10, pp. 326–329, 2011.
- [10] P. Kumar, Z. Akhter, A. K. Jha, and M. J. Akhtar, "Directivity enhancement of double slot Vivaldi antenna using anisotropic zero-index metamaterials," in *IEEE Antennas and Propagation Society Int. Symp. (APS-URSI)*, Vancouver, British Columbia, Canada, pp. 2333–2334, 2015, July 19–24.
- [11] A. Dhouib, S. N. Burokur, A. Lustrac, and A. Priou, "X-band metamaterial-based Luneburg lens antenna," in *IEEE Int. Symp. Antennas and Propagation Society (APS-URSI)*, Orlando, Florida, 2013, July 7–13.
- [12] A. Elsherbini, C. Zhang, S. Lin, M. Kuhn, A. Kamel, A. E. Fathy, and H. Elhennawy, "UWB antipodal Vivaldi antennas with protruded dielectric rods for higher gain, symmetric patterns and minimal phase center variations," in *IEEE Int. Symp. Antennas and Propagation Society (APS-URSI)*, Honolulu, Hawaii, pp. 1973–1976, 2007, June 9–15.
- [13] A. M. Oliveira De, M. B. Perotoni, S. T. Kofuji, and J. F. Justo, "A palm tree antipodal Vivaldi antenna with exponential slot edge for improved radiation pattern," *IEEE Antennas Wirel. Propag. Lett.*, vol. 14, pp. 1334–1337, 2015.
- [14] Y. W. Wang, G. M. Wang, and B. F. Zong, "Directivity improvement of Vivaldi antenna using double-slot structure," *IEEE Antennas Wirel. Propag. Lett.*, vol. 12, pp. 1380–1383, 2013.
- [15] K. S. Yngvesson, T. L. Korzeniowski, Y. S. Kim, E. L. Kollberg, and J. F. Johansson, "The tapered slot antenna-A new integrated element for millimeter-wave applications," *IEEE Trans. Microwave Theory Tech.*, vol. 37, pp. 365–374, 1984.
- [16] E. Gazit, "Improved design of the Vivaldi antenna," *Proc. Inst. Elect. Eng.*, vol. 135, pp. 89–92, 1988.
- [17] D. H. Schaubert, J. A. Aas, M. E. Cooley, and N. E. Buris, "Moment method analysis of infinite stripline-fed tapered slot antenna arrays with a ground plane," *IEEE Trans. Antennas Propag.*, vol. 42, pp. 1161–1166, 1994.
- [18] M. J. Povinelli, "Experimental design and performance of end-fire and conformal flared slot (notch) antennas and application to phased arrays: an overview of development," in *Proc. Antenna Application Symp.*, Allerton Park/Monticello, Illinois, 1988.
- [19] R. M. Barret, "Microwave printed circuits-a historical survey," *IRE Trans. Microwave Theory Tech.*, vol. 3, pp. 1–9, 1955.
- [20] A. Sardi, J. Zbitou, A. Errkik, L. E. Abdellaoui, A. Tajmouati, and M. Latrach, "A novel design of a low cost wideband Wilkinson power divider," *Int. J. Electr. Comput. Energetic Electron. Commun. Eng.*, vol. 9, pp. 68–71, 2015.
- [21] D. M. Pozar, *Microwave Engineering*, 3rd ed. New Delhi: John Wiley & Sons, 2008.
- [22] Z. Akhter and M. J. Akhtar, "Time domain microwave technique for dielectric imaging of multi-layered media," *J. Electromagn. Waves App.*, vol. 29, pp. 386–401, 2015.
- [23] Z. Akhter, B. N. Abhijith, and M. J. Akhtar, "Hemisphere lens-loaded Vivaldi antenna for time domain microwave imaging of concealed objects," *J. Electromagn. Waves App.*, vol. 30, pp. 1183–1197, 2016.